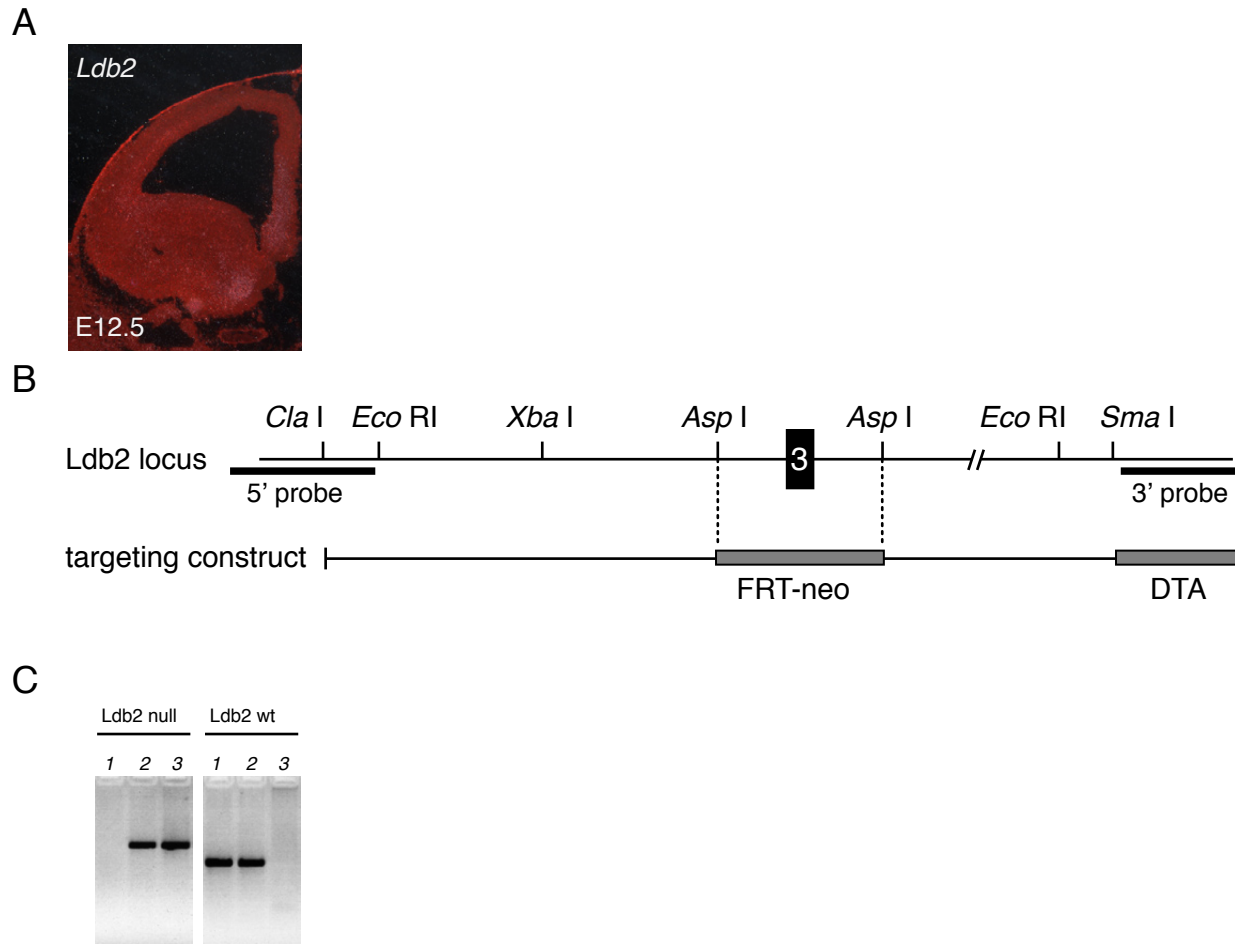


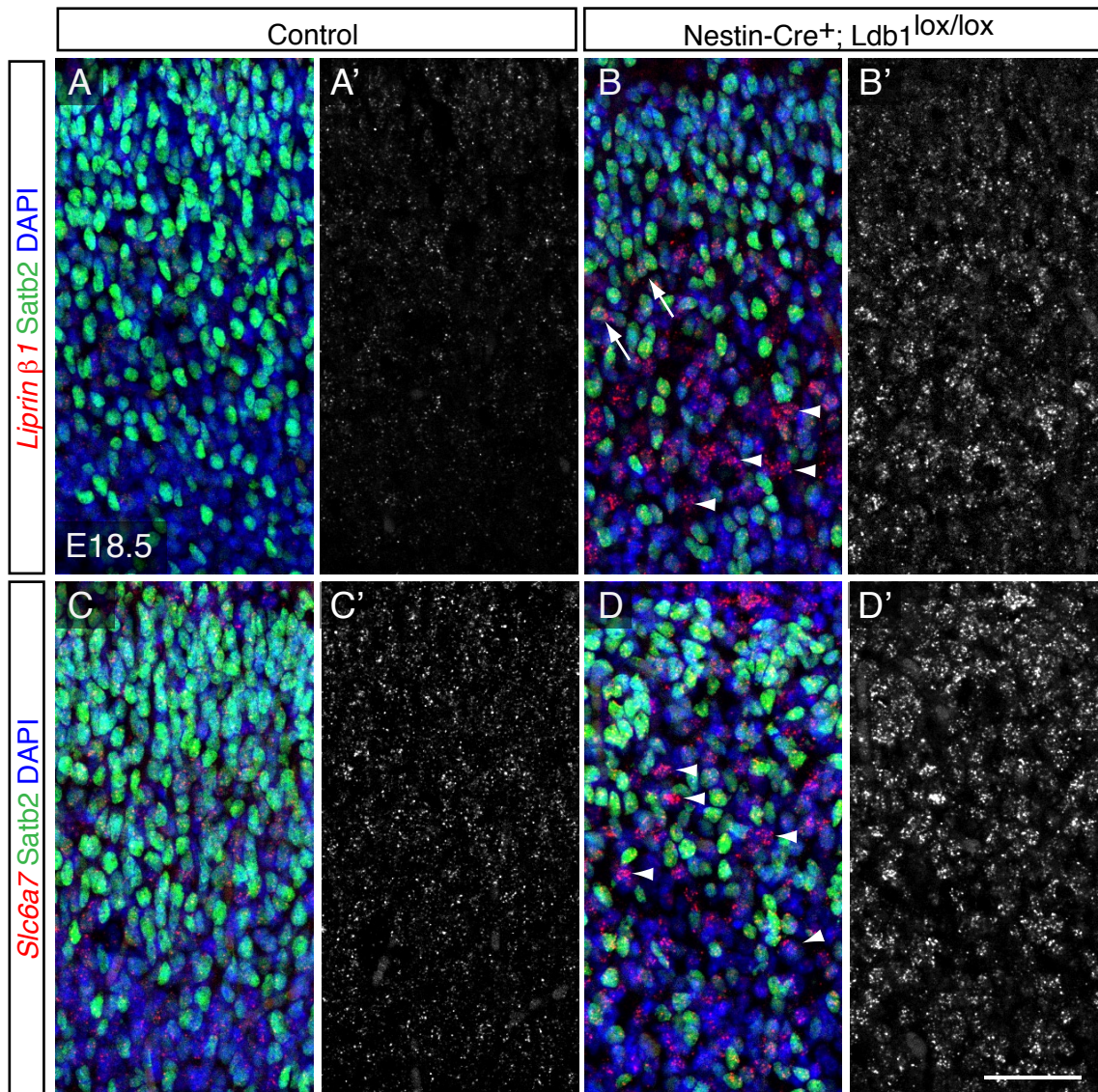
Leone et al., Suppl. Figure 1



Supplementary Figure 1. Early Ldb2 expression and knock-out strategy for Ldb2 null allele.

(A) In situ hybridization at E12.5 for Ldb2 shows no detectable Ldb2 expression in the cortical plate. (B) Schematic drawing of approximately 10 kb genomic Ldb2 locus surrounding exon 3 (boxed, black), which was replaced by a FRT-neo cassette, using AspI sites flanking exon 3. Diphtheria toxin cassette (DTA) served as negative selection against randomly integrated clones. Flanking black boxes indicate probes that were used for Southern blots (5' probe, 3' probe). (C) Genotyping of Ldb2 null animals. Primer pair Ldb2_neo5/Ldb2_neo3 was used for Ldb2 null PCR, and Ldb2_F2/Ldb2_R2 for Ldb2 wt PCR. Sample 1 is a wildtype control, sample 2 a Ldb2^{+/-} heterozygous, and sample 3 a Ldb2^{-/-}.

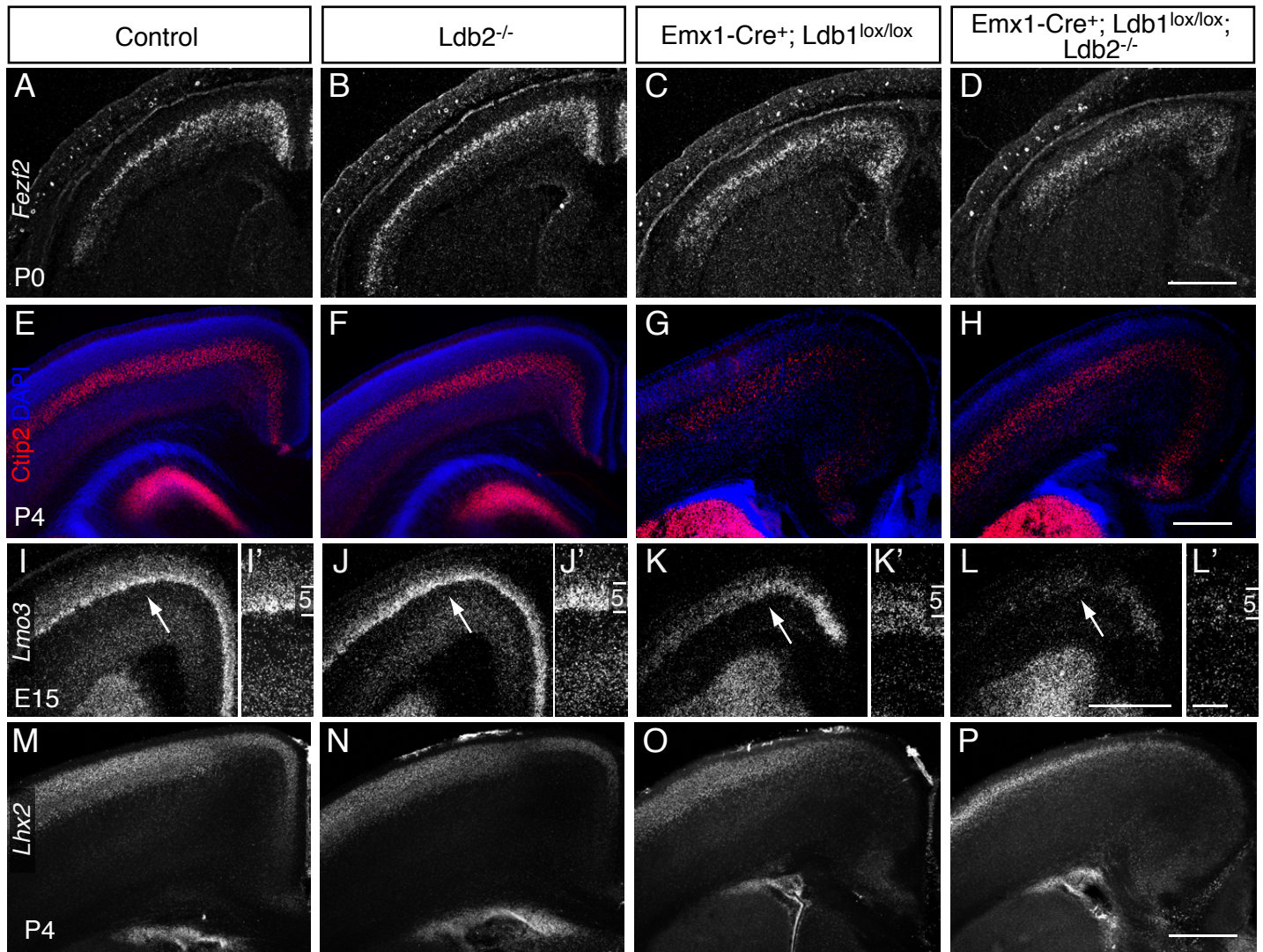
Leone et al., Suppl. Figure 2



Supplementary Figure 2. Regionalization fate change leads to upregulation of piriform cortex markers in dorsal neocortex of *Ldb1*-deficient brains, reminiscent of *Lhx2* knockouts.

High power confocal pictures of E18.5 coronal sections stained with DIG-labeled in situ probes reveal ectopic expression of piriform cortex-specific genes in dorsal neocortex of *Ldb1*-deficient brains. (A-B') Liprin $\beta 1$ (*Ppfibp1*; red in A and B, white in A' and B'), a piriform-specific marker, is not expressed in wild-type E18.5 dorsal neocortex (A, A'), but strongly upregulated in the neocortex of *Ldb1*-deficient brains (B, B'). The vast majority of Liprin $\beta 1$ + cells do not coexpress Satb2 (green in B; arrowheads in B), while a few cells, expressing low levels of Liprin $\beta 1$, can be seen to be coexpressing Satb2 (arrows in B). (C-D') *Slc6a7*, another marker for piriform cortex, shows some basal reactivity in motor cortex of controls (red in C, white in C'), but robust upregulation in *Ldb1*-deficient motor cortex (red in D, white in D'). The majority of high level expressing *Slc6a7*+ cells does not appear to be coexpressing Satb2 (arrowheads in D), suggesting coexistence of piriform and neocortical neurons in *Ldb1*-KO motor cortex. Of note: the Nestin-cre line used here (Petersen et al., Nature, 2002) leads to recombination as early as E8.5. Scale bar: 50 μ m in D' for A-D'.

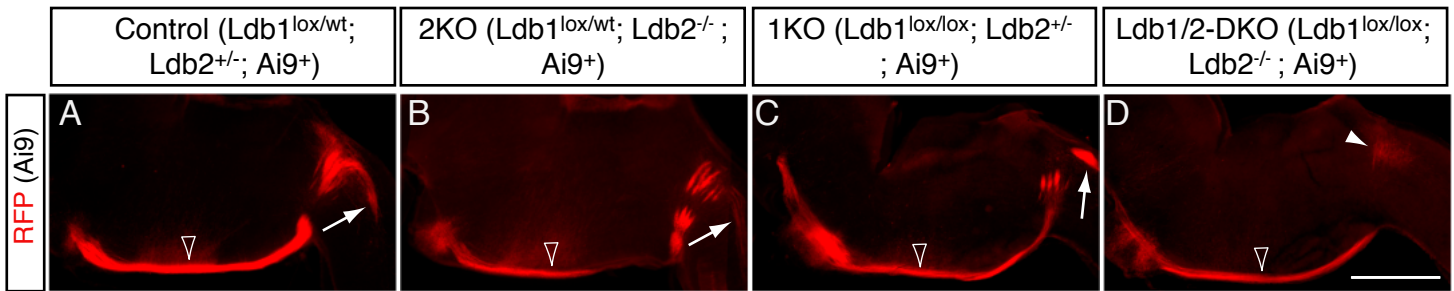
Leone et al., Suppl. Figure 3



Supplementary Figure 3. Specification of CSMN is unaffected by loss of *Ldb1/2*.

(A-D) In situ hybridization for CSMN fate specification marker *Fezf2* at P0 is unchanged in mutants (B-D) compared to controls (A). (E-H) Expression pattern of layer 5 marker *Ctip2* (red in E-H) at P4 appears unchanged in mutants (F-H) compared to control (E). (I-L') In situ hybridization for *Lmo3*, one of the potential interaction factors for *Ldb1/2*, is strongly expressed in layer 5 (arrows in I-L) at E15.5 in controls (I, I') and *Ldb2*-KO (J, J'), qualitatively reduced in *Ldb1*-KO (K, K'), but lost in the neocortex of *Ldb1/2*-DKO (L, L'). Striatal expression is maintained in agreement with the neocortex specificity of *Emx1-Cre*. (M-P) *Lhx2*, one of the major interaction partners of *Ldb* proteins, is expressed by upper layer neurons and its overall expression pattern appears unaffected by loss of *Ldb1/2*. Scale bars: 500 μ m in D (A-D), H (E-H) and in L (I-L); 100 μ m in L' (I'-L'); 500 μ m in P (M-P).

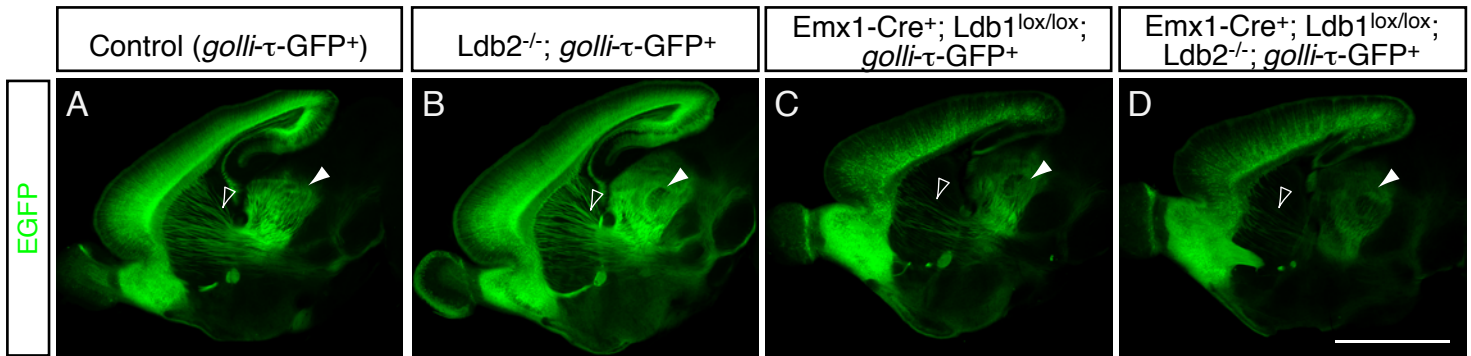
Leone et al., Suppl. Figure 4



Supplementary Figure 4. Cortical CAG-Cre electroporation at E12.5 leads to robust labeling of cortical efferents including the CST on the Ai9 reporter allele and reveals failure of the CST at the pyramidal decussation in Ldb1/2-DKO.

Electroporation of Cre plasmid into the cortical plate at E12.5 and analysis at P5 reveals CST failure in Cre-mediated Ldb1/2-DKO axons labeled by Ai9-RFP. Sagittal sections through the brainstem show RFP labeling in the CST of the medulla (open arrowheads in A-D) of controls (A), Ldb2-KO (B), Ldb1-KO (C) and Ldb1/2-DKO (D). The tracts is shown descending posterior of the pyramidal decussation along the spinal cord (arrows in A-C) of controls, Ldb2-KO and Ldb1-KO, but absent in Ldb1/2-DKO (D). Instead, local axon defasciculation is visible in Ldb1/2-DKO (filled arrowhead in D). Scale bar: 1 mm in D for A-D.

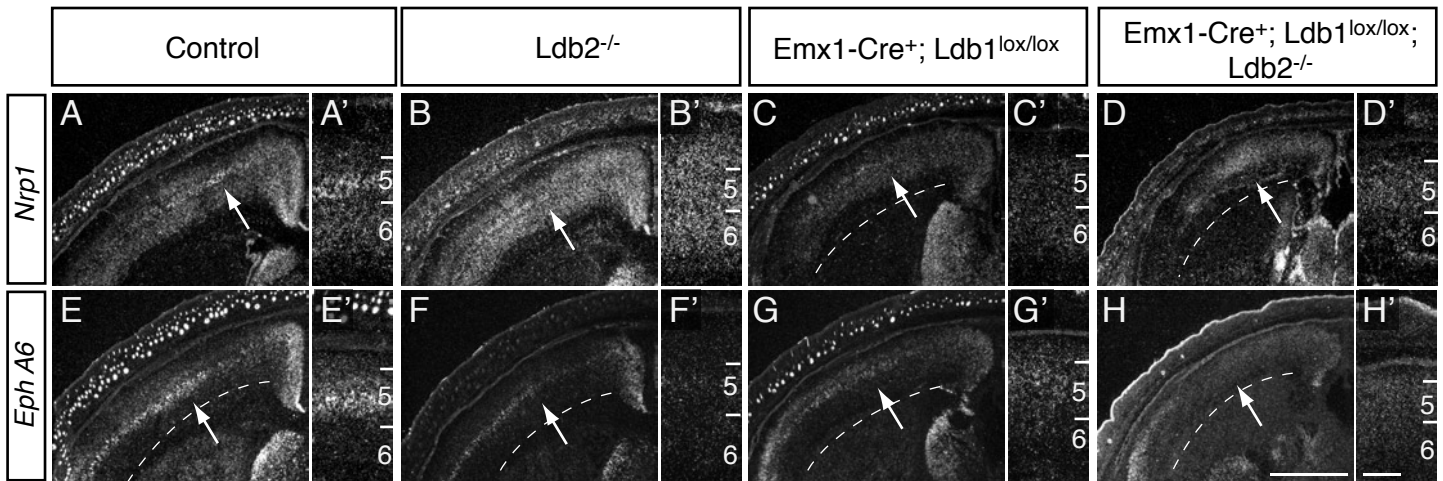
Leone et al., Suppl. Figure 5



Supplementary Figure 5. Corticothalamic projections are unaffected by loss of *Ldb1/2*.

(A-D) *Golli-τ*-EGFP transgene, which labels axons of layer 5 and 6, was used to investigate corticothalamic projections in P4 brains. Robust EGFP⁺ innervation of the thalamus is seen in controls (arrowhead in A) and *Ldb2*-KO (B). Qualitatively reduced thalamic innervation is observed in *Ldb1*-KO (C) and *Ldb1/2*-DKO (D), as apparent by the reduced fiber tract density in the internal capsule (compare open arrowheads in C, D with A, B), most likely due to the reduced number of pyramidal neurons in *Ldb1*-deficient mutants, but overall corticothalamic efferents appear unaffected by the loss of *Ldb1* and/or *Ldb2*. Scale bar: 2 mm in D for A-D.

Leone et al., Suppl. Figure 6



Supplementary Figure 6. Changes in axon guidance receptor expression in Ldb-deficient brains.

In situ hybridization for axon guidance receptors on coronal P1 sections shows defects in axon guidance receptor expression in mutant brains. (A-D') Neuropilin 1 (Nrp1) expression is highest in layer 5 of control brains (arrow in A; A') and Ldb2-KO (B, B'), reduced in Ldb1-KO brains (C, C') and further reduced Ldb1/2-DKO animals (D, D'). (E-H') EphA6 is prominently expressed by layer 5 neurons of controls (arrow in E; E'). Its expression appears reduced in Ldb2-KO brains (F, F') and Ldb1-KO animals (G, G'), and absent in Ldb1/2-DKO brains (H, H'). Scale bars: 1 mm in H for main panels; 0.2 mm in H' for inset panels.